

*Fatigue strength of thermal cut steel edges at  
sub-zero temperatures*

Project Thesis

Submitted by: Marten Beiler  
Student ID Number: 21490774  
Study program: Schiffbau und Meerestechnik  
  
Supervisors: Prof. DSc. (Tech.) Sören Ehlers  
Dr. -Ing. Moritz Braun  
  
Submission Date: July 4th, 2022

## **Abstract**

Openings in the outer shell of ship structures are typically thermal cut. Thermal cut steel edges have an increased risk for fatigue failure due to their local geometry. Additionally the temperature also effects the fatigue strength of thermal cut edges. Since fatigue crack growth testing of base material had shown that the crack growth can be accelerated at low temperatures the effect of low temperatures on thermal cut edges is of particular interest for the fatigue assessment of cruise ships and large yachts, which operates in seasonal freezing temperatures. However the current guidelines for the fatigue assessment of ship structures do not take the effect of low temperatures on the fatigue performance of thermal cut steel edges into account. In order to investigate whether low temperatures have an influence on the fatigue strength of thermal cut steel edges, fatigue tests of plasma cut specimens at  $-20^{\circ}\text{C}$ ,  $-50^{\circ}\text{C}$  and at room temperature are conducted. The results are then statistically evaluated with linear regression and the maximum likelihood method. Thereby it is found that the fatigue strength increase significantly at the tested sub-zero temperatures compared with room temperature. Accordingly no increased risk to fatigue failure of thermal cut steel edges at sub-zero temperatures were found in this thesis.

# Content

- List of Figures ..... iv**
- List of Tables..... v**
- Nomenclature..... vi**
- Abbreviations..... vii**
- 1 Introduction ..... 1**
- 2 Theory..... 2**
  - 2.1 Mechanical properties of steel at sub-zero temperatures ..... 2
    - 2.1.1 Fracture toughness..... 2
    - 2.1.2 Fatigue properties ..... 3
    - 2.1.3 Fatigue properties of welds at sub-zero temperatures ..... 4
  - 2.2 Representation of fatigue test results..... 4
  - 2.3 Statistical methods for the evaluation of fatigue tests ..... 6
    - 2.3.1 Linear Regression..... 6
    - 2.3.2 Maximum likelihood method ..... 7
- 3 Test setup and specimen characterization ..... 9**
- 4 Test results ..... 11**
- 5 Further analyses of the test results ..... 15**
  - 5.1 Fracture surface ..... 15
  - 5.2 Crack position..... 16
  - 5.3 Linear regression with constant slope ..... 18
- 6 Discussion ..... 19**
- 7 Conclusion..... 21**
- References ..... 23**
- Appendix: Modified S-N curves..... 25**

## List of Figures

Figure 1: Characteristic points on the Charpy impact transition curves. Solid line represents impact energy transition curve and dotted line represents fracture appearance transition curve. (taken from [13]).	3
Figure 2: “Schematic S-N curve for steel and metallic materials” with (ND/SaD) as the kneepoint. (taken from [9]).	5
Figure 3: Example for the parameters of a S-N curve with $k$ and $k^*$ as the slopes (taken from [5]).	8
Figure 4: Geometry of tested specimens.	10
Figure 5: S-N curves from linear regression for $-20^{\circ}\text{C}$ (a), $-50^{\circ}\text{C}$ (b) and RT (c).	13
Figure 6: S-N curves from maximum likelihood method for $-20^{\circ}\text{C}$ (a), $-50^{\circ}\text{C}$ (b) and RT (c).	15
Figure 7: Fracture surface of specimens tested at temperatures of $-50^{\circ}\text{C}$ (a), $-20^{\circ}\text{C}$ (b) and at RT (c).	16
Figure 8: S-N curve for test results at $-50^{\circ}\text{C}$ with modified stress ranges evaluated with the maximum likelihood method. The white triangle shows the outlier.	17
Figure 9: Increase of the FAT-class value in percent of original test series at sub-zero temperatures compared to RT and of modified test series compared to RT modified.	19

## List of Tables

Table 1: Chemical composition in % of AH36 and mechanical properties. ....	10
Table 2: S-N curve parameter evaluated with linear regression and with maximum likelihood method for all test series.....	18
Table 3: FAT-class values for test series RT, -20°C and -50°C and for test series with modified stress range values with different fixed slopes and FAT-class values from guidelines [1, 8].....	18

## Nomenclature

$N$		Number of cycles
$N_k$		Number of cycles at knee point
$S_k$	MPa	Stress range at knee point
$S$	MPa	Stress range
$m$		Slope of S-N curve in linear regression
$n$		Number of data pairs
$stdv(\lg C)$		Standard deviation of logC in DVS recommendation
$T_s$		Scatter ratio in strength
$P_{tot,max}$		Highest probability of occurrence
$P_i$		Probability of occurrence for one test point
$P_{i=1,fail}$		Probability of occurrence for a failure
$P_{i=2,runout}$		Probability of occurrence for a runout
$stdv$		Standard deviation in the direction of the stress range
$sup_1$		Support function for $N_i < N_k$
$sup_2$		Support function for $N_i > N_k$
$sup_B$		Support function for runout
$m_1$		Slope before the knee point in maximum likelihood method
$m_2$		Slope behind the knee point in maximum likelihood method
$T_{27J}$	°C	Temperature at which the Charpy impact energy is 27J
$T_0$	°C	Temperature at which the $K_{Ic}$ is $100MPa\sqrt{m}$

## Abbreviations

IIW	International Institute of Welding
DNV	Det Norske Veritas (Classification society)
DVS	Deutscher Verband für Schweißen und verwandte Verfahren
RT	Room temperature
HCF	High cycle fatigue regime
LCF	Low cycle fatigue regime
LLF	Long life fatigue regime
DBTT	Ductile to brittle transition temperature
FATT	Fracture-appearance transition temperature
FDBT	Fatigue Ductile-Brittle Transition
FTT	Fatigue transition temperature
FCG	Fatigue crack growth
CTOD	Crack tip opening displacement
LAST	Lowest anticipated service temperature

# 1 Introduction

Sub-zero temperatures influence the fatigue strength of ship structures. Beside of root and toe failure of welds, free thermally cut steel edges are also critical details in the ship structure for crack initiation under cyclic loading. Especially the ship hull of modern cruise ships and large yachts consists of a recent number of openings for windows and balcony doors. When this kind of ships operate in arctic conditions those cutouts are exposed to very low air temperatures, which leads to a change in their fatigue behavior.

The fatigue performance of free plate edges is researched for normal temperatures and also the effect of high temperatures are already well known. Accordingly current standards like the recommendation of the IIW provide a factor for fatigue assessment at high temperatures which depends on the modulus of elasticity [1]. But the researches for sub-zero temperatures are scarce. In comparison to that the fatigue strength of fillet welds at sub-zero temperatures is already investigated by Braun et al. [2]. In that study it is found that the fatigue strength of fillet welds increases at low temperatures up to  $-50^{\circ}\text{C}$ . This founding shows that normal and higher strength steels are better suited for arctic environment then previous studies assumed on the base of fracture toughness tests.

To extend the knowledge of the effect of sub-zero temperatures on fatigue performance of critical details in ship structures free thermal cut steel edges are tested in this thesis. For this purpose plasma cut specimens are tested at room temperature (RT),  $-20^{\circ}\text{C}$  and  $-50^{\circ}\text{C}$ . Then the test results are statistical evaluated to find the best fit S-N curves for the results of each test temperature. On the base of the best fit S-N curves (Wöhler curve), to describe the fatigue performance of the specimens at certain temperatures, the test results can be compared

## 2 Theory

### 2.1 Mechanical properties of steel at sub-zero temperatures

When steels are exposed to an environment with sub-zero temperatures like in ships or offshore structures in the arctic, the safety of the application depends among others on the changes of material properties at low temperatures. While the current guidelines focus on fracture toughness to avoid brittle fracture the effect of sub-zero temperatures on the fatigue properties of steel are ignored. [11]

#### 2.1.1 Fracture toughness

Ferritic structural steels with a body-centered cubic crystal structure have a reduced fracture toughness at low temperature. While at higher temperatures the fracture mode is shear-dominated (ductile) the fracture mode changes to a cleavage or intergranular fracture-dominated (brittle) one. This makes brittle fracture one major risk for steel structures at sub-zero temperatures. To counter this, a sufficient high fracture toughness is required from the guidelines of the classification societies. [14]

The fracture toughness can be measured through different fracture mechanical tests. Commonly used is the Charpy V-notch impact toughness tests (Charpy test), but also three point bending tests (CTOD testing) to determine the crack tip opening displacement CTOD, the critical stress intensity factor  $K_{Ic}$  or J-Integral testing are applied. The transition from the ductile fracture behavior of the steel to the brittle fracture behavior is characterized by the Ductile to Brittle Transition Temperature (DBTT). In the guidelines of the classification societies it is required that the steels DBTT has to be below the Lowest Anticipated Service Temperature (LAST), to ensure that no brittle fracture occur. However, the definition of the DBTT is not fixed linked to a certain measure. Commonly this temperature is determined by conducting Charpy test on a wide temperature range. The measure for the DBTT is in this case the  $T_{27J}$  temperature at which the specimen yields energy of 27J. This amount of absorbed energy corresponds for many structural steels to the lower end of the transition region and is close to the lower shelf of the Charpy impact transition curve. But other measures are used as well like the fracture-appearance transition temperature (FATT) where 50% of the fracture surface shows a characteristic brittle fracture. Moreover also the  $T_0$  temperature evaluated with CTOD testing can be used as a measure of the DBTT. At this temperature a specimen have a  $K_{Ic}$  of  $100MPa\sqrt{m}$ . Despite the fact that the parameters are independent from each other, it is known that the FATT is tending to be higher than the  $T_{27J}$ . Furthermore  $T_0$  tends to be approximately

18°C below the  $T_{27J}$ . The temperature difference between FATT and the  $T_{27J}$  is shown schematically in Figure 1. [12] [14]

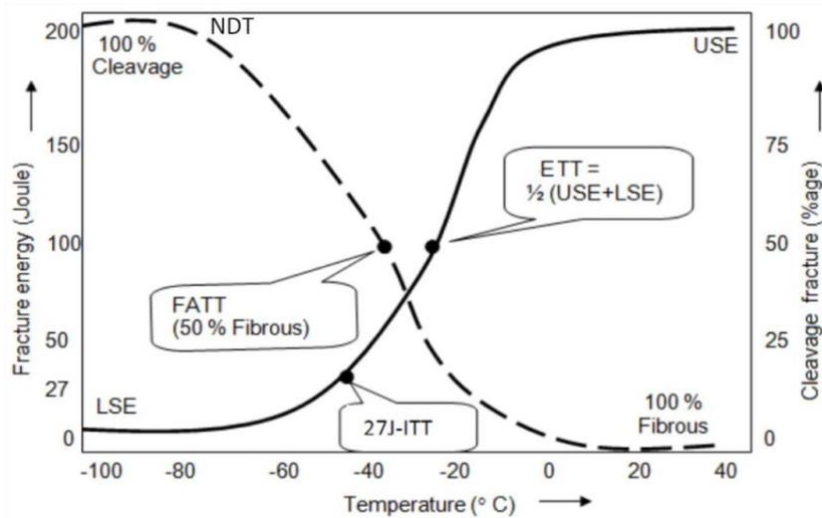


Figure 1: Characteristic points on the Charpy impact transition curves. Solid line represents impact energy transition curve and dotted line represents fracture appearance transition curve. (taken from [13]).

In the maritime industry the parameters evaluated with the Charpy V-notch impact toughness test are most common. Thereby the  $T_{27J}$  is more popular than the FATT. In some cases, next to the  $T_{27J}$ , the temperature at which a specimen absorbs an energy of 10% of the yield strength in MPa in joule in the Charpy test is used. Parameters evaluated with CTOD-testing are in general only used when a material fails the Charpy test requirements. [14]

### 2.1.2 Fatigue properties

In comparison to the effect of sub-zero temperatures on the fracture toughness, changes of the fatigue properties at low temperatures of steel are not considered in the current guidelines for steel structures like DNV or IIW. Thereby the assumption that sub-zero temperature in the range of the ships polar service temperatures have no detrimental effect on the fatigue properties of steel is based on fatigue crack growth testing of base material. [11]

The crack initiation and the crack propagation occur under cyclic loading through non detectable dislocation movements at notches, material defects, and grain boundaries [11]. At low temperatures the dislocation movement is inhibited through which the steel's resistance against crack initiation and propagation increases. However similar to the ductile to brittle transition of fracture toughness also fatigue undergoes a transition at low temperatures. This transition is called the Fatigue Ductile-Brittle Transition (FDBT). The crack growth is accelerated when the temperature is below the so called fatigue transition temperature (FTT)

which characterizes the transition. This temperature is in the range of the ductile to brittle transition and lies below the FATT but is in general higher than the  $T_{27J}$  temperature. The fatigue crack growth (FCG) rate is higher below the FTT, than above, but the fatigue crack growth is not so much accelerated that the FCG is higher than it is at RT. This has been showed by tests with weld thermal simulated homogeneous steel samples. [11 - 14]

### 2.1.3 Fatigue properties of welds at sub-zero temperatures

The material properties of steel at sub-zero temperatures are well investigated for plain steel specimens. However, one critical structural detail in terms of fatigue in ship structures are welds. The fatigue design of welds in ships and offshore structures are based on S-N design curves. As for this topic a major knowledge gap existed, current studies from Braun et al. focus on the investigation of the fatigue strength of fillet-welded joints [2] and butt welds [15] at subzero temperatures. The aim of that studies was to investigate S-N data for different steel types at sub-zero temperatures and to “assess the effect on fatigue assessment procedures for structures experiencing low service temperatures” [2]. In both of the studies no decrease in fatigue strength up to  $-50^{\circ}\text{C}$  was found in comparison to room temperature. Instead an increase in fatigue strength up to 31.1% for butt welded joints and up to approximately 22% for filled-welded joints were observed. Through this studies it is shown that some standards are very conservative and that welded joints can be safely applied to sub-zero temperatures down to  $-50^{\circ}\text{C}$ .

## 2.2 Representation of fatigue test results

The results of fatigue tests are represented by S-N curves. A common representation of S-N curves is to plot the number of cycles to failure logarithmically on the abscissa and the stress range logarithmically on the ordinate. In order to derive the S-N curve, samples of the same material, preparation and size are subjected to a sinusoidal vibration load which is characterized by its stress range  $\Delta\sigma$  and a constant stress ratio R. When a specimen reaches the previously defined failure criterion (crack initiation or breaking) the cycles to failure are noted whereby one datapoint, which is needed to calculate the S-N curve is against. In case the specimen doesn't fail at the chosen stress range this test is marked as a runout. For that number of cycles where the test is stopped is specified before. [3] [4]

In order to be able to compare fatigue test results, the parameters of the S-N curves has to be investigated. Three different regions in S-N curves are distinguished, the Low cycle fatigue regime (LCF) the high cycle fatigue regime (HCF) and the long life fatigue regime (LLF). To However to investigate the fatigue strength of steel specimens the focus is on the HCF and the

LLF. The HCF is represented by a straight line. At a certain stress range this line is getting less steep which marks the transition to the LLF. The position where the slope of the curve change is represented by the knee point. A schematic S-N curve is shown in Figure 2.

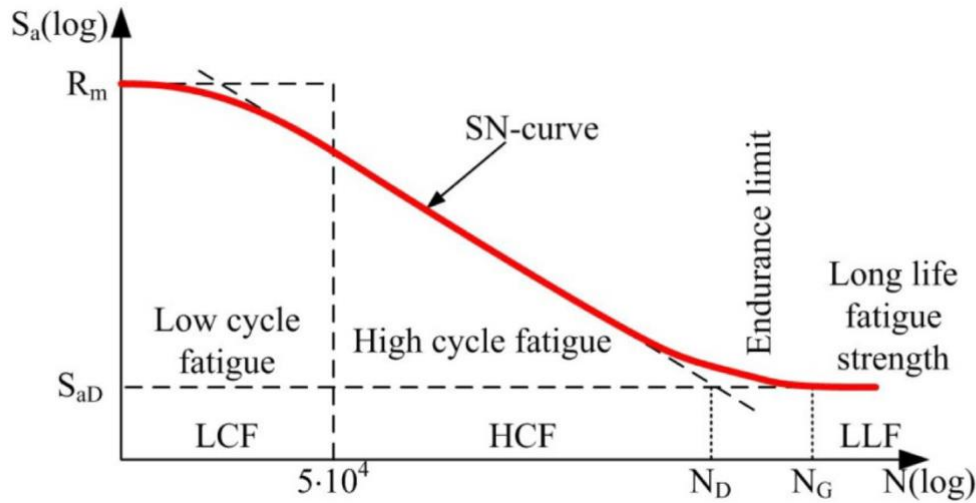


Figure 2: “Schematic S-N curve for steel and metallic materials” with  $(N_D/S_{aD})$  as the kneepoint. (taken from [9]).

The straight line in the high cycle fatigue regime is described by the logarithmic Basqiuin-Equation [4]

$$\lg N = \lg N_k \cdot S_k^m + m \cdot \lg S \quad (1)$$

In the Equation, N is the number of cycles,  $N_k$  the number of cycles at the knee point,  $S_k$  the nominal stress range level at the knee point, S the reference fatigue stress and m the slope exponent of the curve. The slope exponent is typically a negative value in the range of  $-2.5 \leq m \leq -20$ . Parameters for describing the S-N curves are the slope exponent in the high cycle fatigue regime and the transition to the long life fatigue regime. [4] [5]

The testing procedure is about to investigate the parameters. For that different methods can be used. One way of testing is to conduct some tests at two different load levels (load-level method). Thereby the datapoints scatters at one load level which is attributed to differences in the material. A good approximation to describe the scatter at one load level is the logarithmic normal distribution. To find the slope of the S-N curve the mean value at both load levels are calculated. The disadvantage of this way of testing is that a relatively large number of specimens is needed. Because of that the pearl string method is better suited in case only a small number of specimen is available. With this method tests are carried out at different load levels along the straight line in the high cycle fatigue regime. Then the S-N curve is evaluated using statistical methods. [4] [5]

## 2.3 Statistical methods for the evaluation of fatigue tests

Statistical methods are used for evaluation of fatigue tests which are carried out with the pearl string testing procedure. In that case the datapoints are available along the straight line in the high cycle fatigue regime. To determine the best fit S-N curve from that data, a line which follows the logarithmic Basqiu Equation has to be found. This can be done in two different ways. On one hand linear regression is used to evaluate the S-N curve by minimization of the distances in the direction of cycles. On the other hand the best fit S-N curve can be evaluated by using the maximum likelihood method which is about to find the bilinear S-N curve with the highest probability of occurrence. [4]

### 2.3.1 Linear Regression

The method of linear regression for the evaluation of fatigue test results is recommended by the DVS (Deutscher Verband für Schweißen und Verwandte Verfahren e.V.) [4]. With this method all test data which is available before the knee point are considered. Because of that the knee point is specified according to the fatigue test results, experience and the common ruleset. The high cycle fatigue regime is represented by the logarithmic Basqiu Equation (Equation 1). With the cycles to failure logarithmically on the abscissa and the stress range on the ordinate it can be stated, that the cycles to failure depends linear on the stress range. This is described by Equation 2

$$y = a \cdot x + b \quad (2)$$

with x as the logarithmic stress range and y as the logarithmic cycles to failure.

$$x = \lg \Delta \sigma \quad (3)$$

$$y = \lg N \quad (4)$$

To simplify the notation of the Basqiu Equation (Equation 5), the constant C is introduced.

$$N = C \cdot S^m \quad (5)$$

$$C = N_k \cdot S_k^m \quad (6)$$

As mentioned before it is assumed that the scatter is described by the logarithmic normal distribution. Moreover the scatter is assumed to be constant independent of the load level. Then the slope exponent m can be calculated with Equation 7 and the logarithm of C with Equation 8, where n is the number of data pairs.

$$m = \frac{\sum xy - \frac{\sum x \cdot \sum y}{n}}{\sum x^2 - \frac{(\sum x)^2}{n}} \quad (7)$$

$$\lg C = \frac{\sum y}{n} - m \cdot \frac{\sum x}{n} \quad (8)$$

With the help of the slope  $m$  and the logarithm of  $C$  the S-N curve for a survival probability of 50% in HCF can be derived from Equation 9.

$$S = C \cdot N^{-\frac{1}{m}} \quad (9)$$

For the comparison of fatigue test results it can be interesting to get a measure of the scatter. A measure for the scatter is given by the standard deviation. The standard deviation can be calculated, with the residue square in Equation 10, according to Equation 11.

$$\sum dy^2 = \sum (\lg C + m \cdot x - y)^2 \quad (10)$$

$$\text{stdv}(\lg C) = \sqrt{\frac{\sum dy^2}{n - 2}} \quad (11)$$

The scatter ratio in strength which describes the band width in the direction of the stress range between the line of 90% and 10% survival probability is shown in Equation 12.

$$1: T_s = 10^{-2.56 \frac{\text{stdv}(\lg C)}{m}} \quad (12)$$

With this statistical method the line in the high cycle fatigue regime is calculated up to the knee point. Thereby the runouts are not considered in the evaluation.

### 2.3.2 Maximum likelihood method

Another statistical method for the evaluation of fatigue test results is the maximum likelihood method. This method is also recommended by the DVS [4]. With this method the runouts can be integrated into the evaluation which can lead to better suited S-N curves for the data, especially when the number of specimens is small. The method is about to find the bilinear S-N curve with the highest probability of occurrence from the data. As it is shown by Störzel et al. [5], the maximum likelihood method for fatigue test evaluation leads to reliable parameters of the S-N curve. Different to the linear regression, the S-N curve in the maximum likelihood is represented by a bilinear curve. The curve parameters for the bilinear S-N curve are:

- slope in the high cycle fatigue regime  $m_1$
- stress range at the knee point  $S_k$
- standard deviation  $\text{stdv}$ , as a measure of the scatter in the direction of the stress range
- cycles to failure at the knee point  $N_k$
- slope in the long life fatigue regime  $m_2$

The knee point and the slope in the long life fatigue regime are specified for the calculation and the other three parameters are determined by optimization. The optimization is about to find the highest probability of occurrence for the test points  $i$  ( $S_i, N_i$ ). [5]

$$P_{tot,max} = \max \left( \prod_{i=1}^n P_i \right) \quad (13)$$

In Equation 13,  $P_i$  can be the probability of a test result which failed or which is a runout. As in this method the scatter is described by the logarithmic normal distribution the probability for a failure and for a runout are shown in Equation 14 and 15.

$$P_{i=1,fail} = \frac{1}{stdv \cdot \sqrt{2 \cdot \pi}} \cdot e^{-0.5 \cdot \left( \frac{\lg(y_i) - \lg(y(x_i))}{stdv} \right)^2} dy \quad (14)$$

$$P_{i=2,runout} = \frac{1}{\sqrt{2 \cdot \pi}} \int_{t_i}^{\infty} e^{-0.5 \cdot t^2} dt \quad (15)$$

$$\text{with: } t_i = \frac{(\lg(y_i) - \lg(y(x_i)))}{stdv} \quad (16)$$

It is further assumed that the scatter is independent of the cycles to failure and that the width of the scatter band is constant at the entire S-N curve. Furthermore it is prerequisite for the application of the maximum likelihood method, that lines of the same probability meet in the knee point. Then the bilinear S-N curve looks like it is shown in Figure 3.

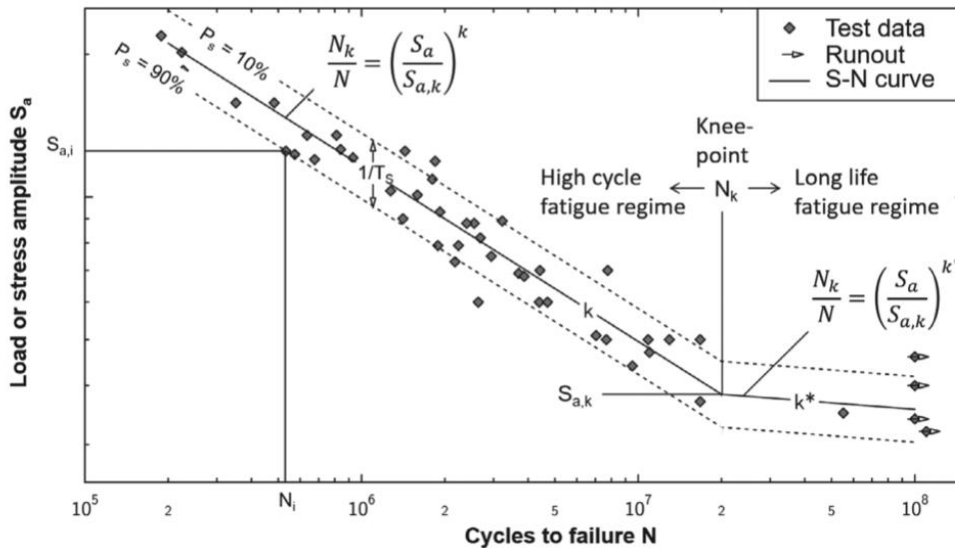


Figure 3: Example for the parameters of a S-N curve with  $k$  and  $k^*$  as the slopes (taken from [5]).

To find the highest probability of occurrence for the parameter of the S-N curve, not the probability of occurrence is optimized but their natural logarithm, as this makes the calculation

easier and leads to the same result for the maximum [5]. These functions are then called support functions (sup). However not only the maximum of one support function leads to the best fit S-N curve. The data can be distinguished into three different groups which depends on the relative position to the knee point:

- Specimens which failed before the knee point ( $N_i < N_k$ )
- Specimens which failed behind the knee point ( $N_i > N_k$ )
- Specimens which doesn't fail (runouts)

For all of the three groups the support function is different. Because of that the maximization of the probability of occurrence has to take all support functions into account to find the best fit S-N curve which is represented by Equation 17.

$$\ln P_{tot,max} = \max(sup_1 + sup_2 + sup_B) \quad (17)$$

The support functions evaluate the distance between the test point and the S-N curve from the regression line in the direction of the stress range. As the slope of the S-N curve is different before and behind the knee point this has to be considered for the support functions. Then the Equation for the support functions that are optimized have the following form. [4]

$$\text{For } N_i < N_k \quad sup_1 = \sum_{n_1} \left( \frac{(-0.5 \cdot (\lg(y_i) - \lg(y(x_i))))^2}{stdv^2} - \ln(m_1 \cdot stdv) \right) \quad (18)$$

$$\text{For } N_i > N_k \quad sup_2 = \sum_{n_2} \left( \frac{(-0.5 \cdot (\lg(y_i) - \lg(y(x_i))))^2}{stdv^2} - \ln(m_2 \cdot stdv) \right) \quad (19)$$

$$\text{For runouts} \quad sup_B = \sum_{n_B} \ln \frac{1}{\sqrt{2 \cdot \pi}} \cdot \int_{t_i}^{\infty} e^{-0.5 \cdot t^2} dx \quad (20)$$

The parameters that are optimized are  $stdv$ ,  $m_1$  and  $S_k$ . This happens through variate these parameters and calculate then the maximum of the support functions according to Equation 17. Because of numerical reasons the knee point can't be optimized together with the other parameters [5]. The only way to do this is to optimize the knee point before optimizing the other parameters. For that Equation 17 is calculated and then maximized for varying knee points. Then the knee point with the highest probability of occurrence is chosen. The band width can then be calculated according to Equation 12 but with the optimized parameters.

### 3 Test setup and specimen characterization

To investigate the fatigue performance of thermal cut steel edges at sub-zero temperatures specimens for test series at RT, -20°C and -50°C are produced. All specimens are made of higher strength construction steel S355 (AH36) and are cut out of one plate by plasma cutting.

The chemical composition of the used steel and the mechanical properties are listed in Table 1. As the plasma cutting is conducted at a yard without special set ups the parameters of the cutting process corresponds to ship building practice. The specimens are 500mm long and 80mm width at both ends with a thickness of 12.5mm. In the center of the specimens the width is reduced to 30mm by a radius of 500mm at both sides through which the specimens have a hourglass like shape (see Figure 4).

Table 1: Chemical composition in % of AH36 and mechanical properties.

<b>C</b>	<b>Si</b>	<b>Mn</b>	<b>P</b>	<b>S</b>	<b>Al</b>	<b>N</b>
0.09	0.25	1.16	0.017	0.006	0.028	0.007
<b>Cr</b>	<b>Cu</b>	<b>Ni</b>	<b>Ti</b>	<b>V</b>	<b>Nb</b>	<b>Mo</b>
0.09	0.22	0.12	0.001	0.001	0.024	0.001
<b>CEV</b>	<b>Tensile Strength</b> $R_m$ [MPa]	<b>Yield Strength</b> $R_{eh}$ [MPa]	<b>Failure Strain</b> [%]			
0.32	538	423	29.2			

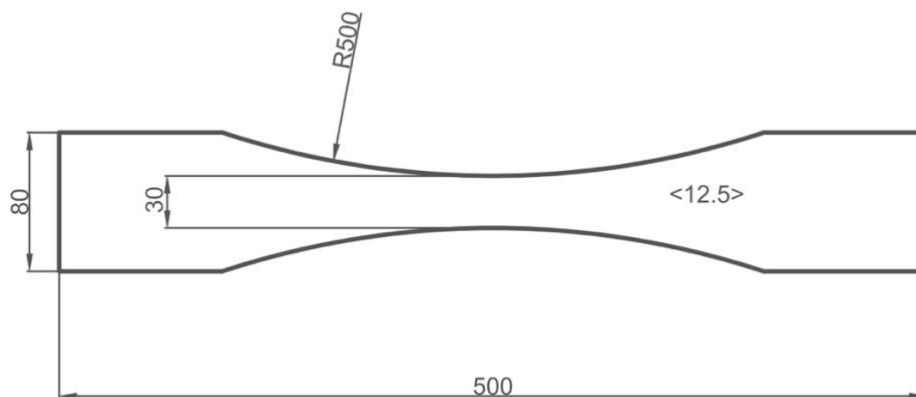


Figure 4: Geometry of tested specimens.

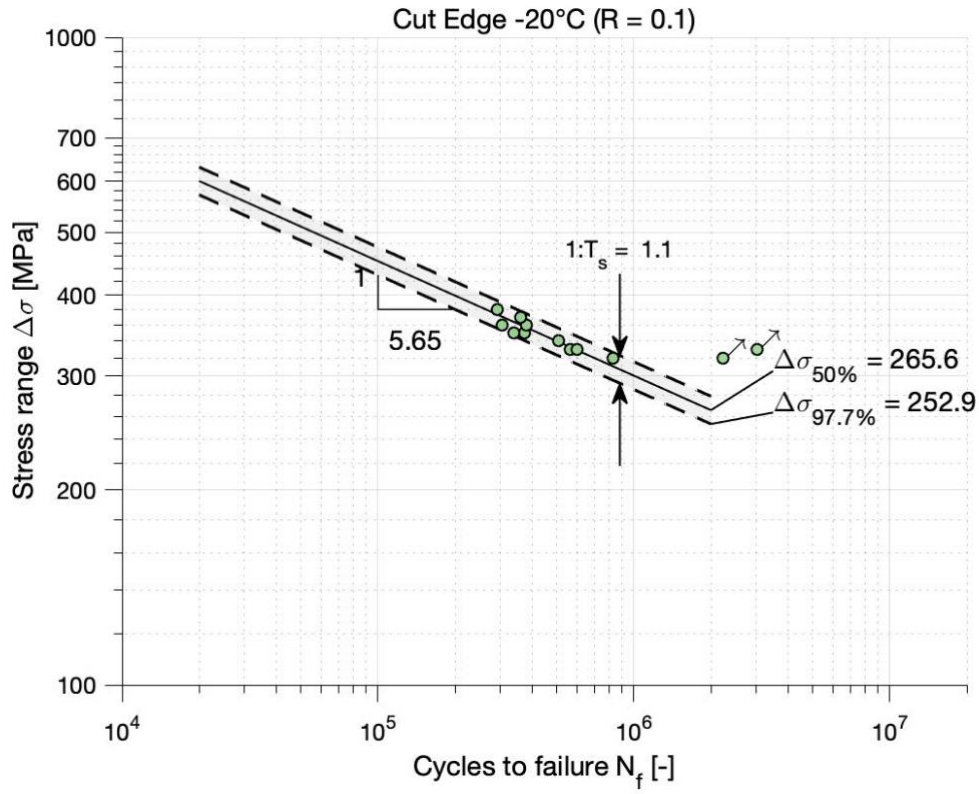
Before the testing start the specimens are characterized. For this the geometry of the smallest area in the center is measured as well as the angular misalignment. The surface roughness is not measured as previous studies shows that the fatigue performance depends more on the cut edge defects and the cutting process as on the roughness [6]. Especially in case of plasma cutting, surfaces with low roughness values are produced, whereby the roughness plays a secondary role [7].

For the fatigue testing of the specimens a Schenk horizontal resonance testing machine is used. The maximum load capacity of the machine is 200kN at a frequency of 33Hz and a stress ratio of  $R=0$ . All tests are conducted with a stress ratio of  $R=0.1$  and the failure criterion is crack initiation. During the testing cooling is achieved by vaporized nitrogen which is blown into a temperature chamber. For an almost constant temperature ( $\pm 1^\circ\text{C}$ ) during the tests the amount of nitrogen is controlled by a temperature gauge. Additionally the temperature in the chamber and of the specimen is recorded by temperature gauges as well.

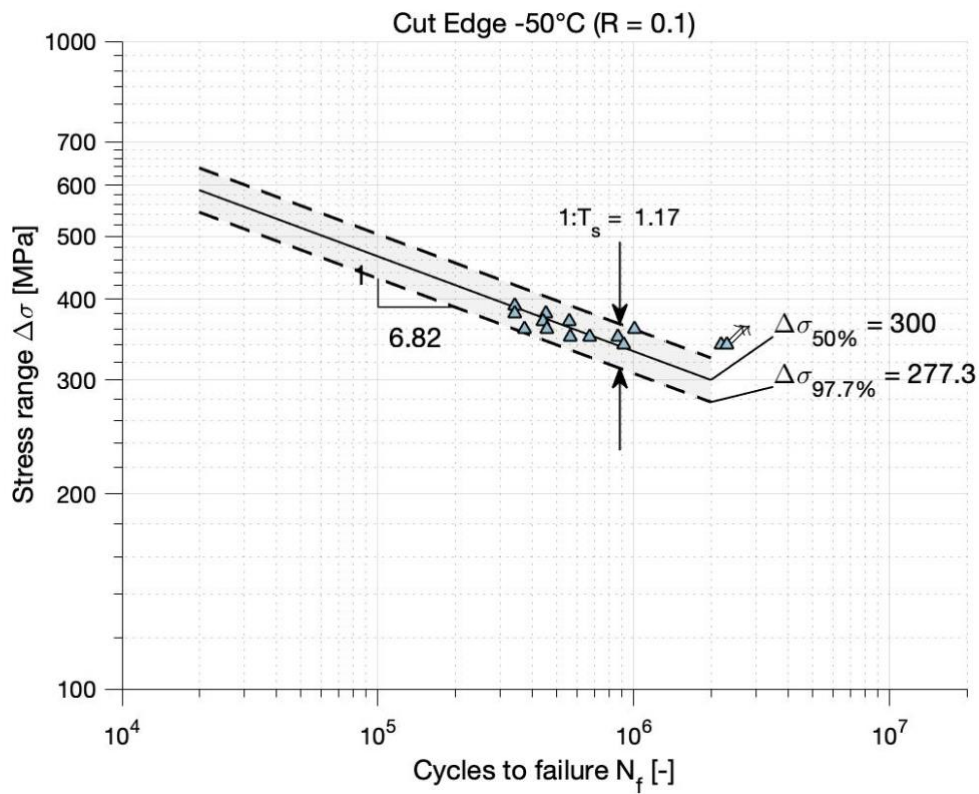
As the number of specimens for each temperature is limited, the pearl string method is used. Here the tests are carried out at different load levels. But at least 10 specimens are tested for each temperature. This is important as a certain number of datapoints are needed for the statistical evaluation of the test results.

#### 4 Test results

To compare the fatigue test results for the different temperature to each other a statistical evaluation is conducted. Thereby both statistical methods which are described before are applied. By using the linear regression the slope in the high cycle fatigue regime is calculated as well as the stress range at  $2 \cdot 10^6$  cycles for 50% - and 97.7% survival probability. This number of cycles is chosen, as here the FAT-class values are available. Moreover the band width of the scatter between 97.7% and 2.3% is derived. In case a specimen doesn't fail before  $2 \cdot 10^6$  cycles are reached those runouts are marked with an arrow. The results for all three test temperatures are shown in the following Figures 5a-5c:



**(a)**



**(b)**

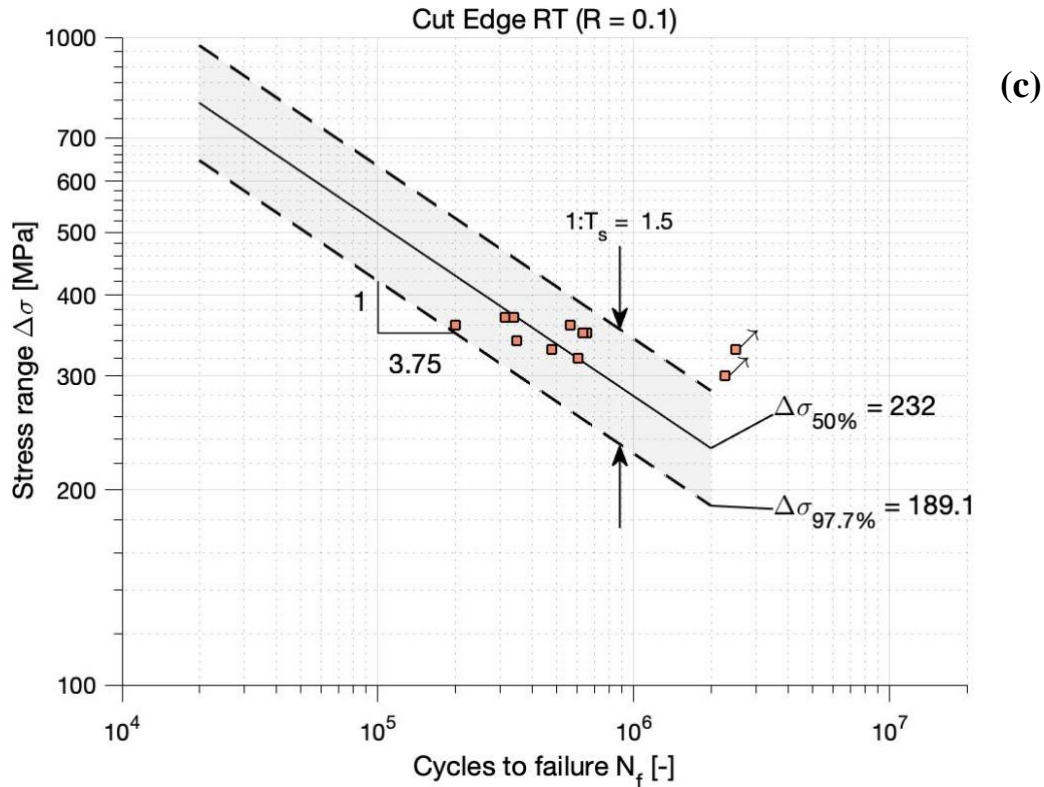
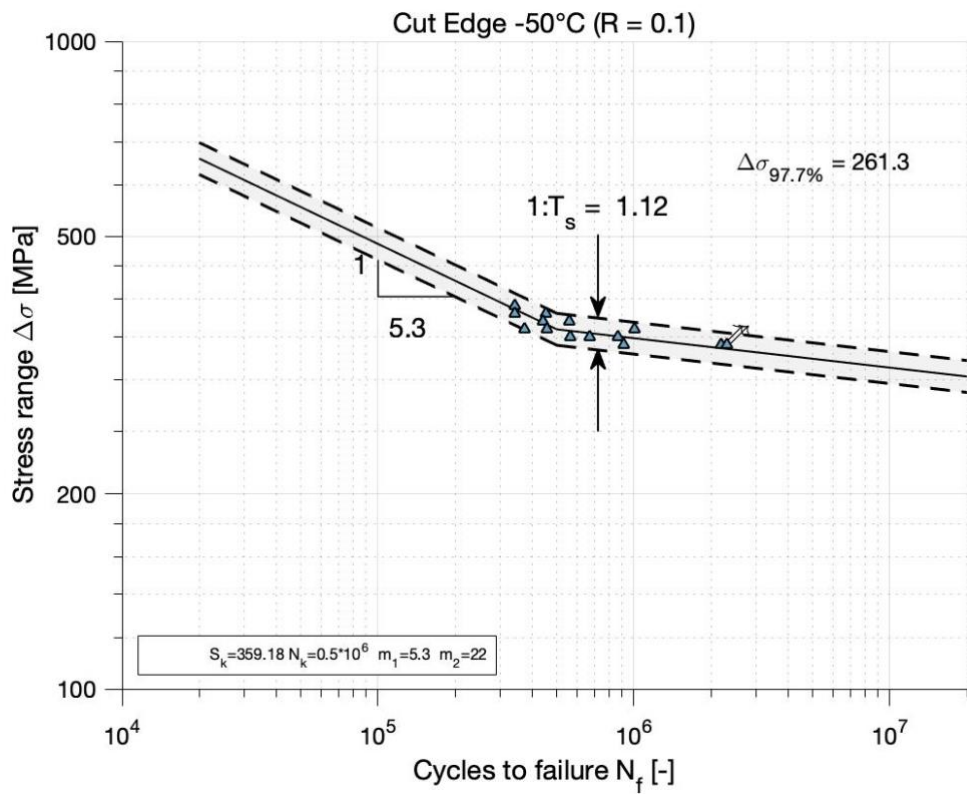
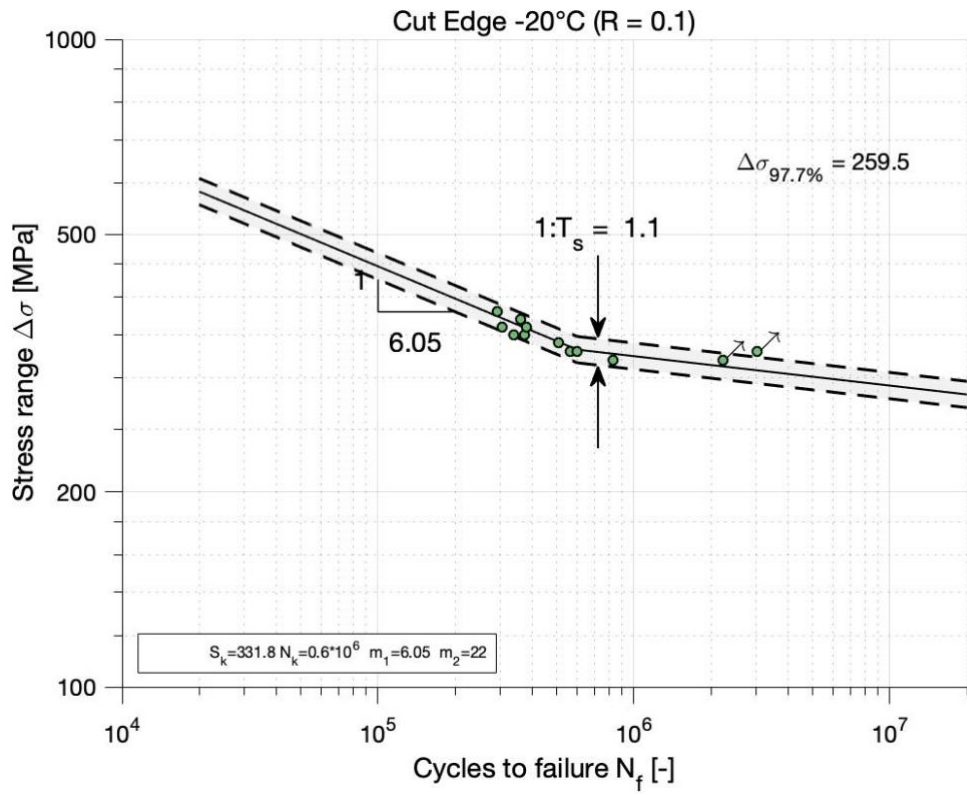


Figure 5: S-N curves from linear regression for  $-20^\circ\text{C}$  (a),  $-50^\circ\text{C}$  (b) and RT (c).

When looking at the S-N curves for different temperatures, it can be observed that the fatigue strength increases with decreasing temperature. The scatter is much higher at RT compared to the sub-zero temperatures. As the slope for RT differs strongly, the algorithm seems not so well suited for data with a high scatter when only a small number of specimens are tested.

Because of that and the fact that the method of linear regression doesn't take the runouts into account the maximum likelihood method is applied to the test results too. As it is shown by Störzel et al. [5] the maximum likelihood method delivers reliable results for all S-N curve parameters even if the number of specimens is limited. First the knee point is optimized by varying  $N_k$  from  $0.5 \cdot 10^6$  up to  $2 \cdot 10^6$  in steps of  $0.1 \cdot 10^6$ . Finally the knee point is chosen, for which the test results have the greatest probability of occurrence. The fixed slope in the high cycle fatigue regime is set to  $m_2=22$  according to the recommendation of DVS [7]. Although the scatter index between 97.7% and 2.3% survival probability, the resulting FAT-class value, the stress range for 50% survival probability at the knee point and the slope  $m_1$  are calculated. The results of the statistical evaluation with the maximum likelihood method are shown in Figures 6a-6c.



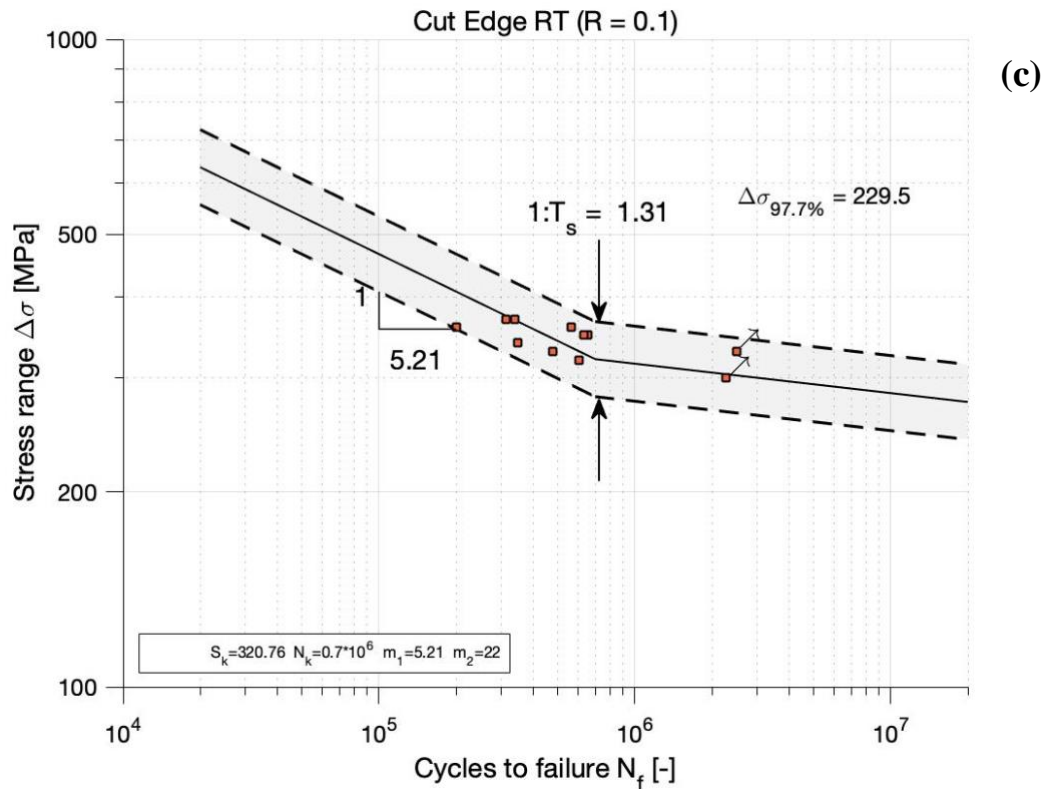


Figure 6: S-N curves from maximum likelihood method for -20°C (a), -50°C (b) and RT (c).

The evaluation with the maximum likelihood method confirms to the increase in fatigue strength by decreasing temperatures but the differences are smaller. Even if the stress range for a survival probability of 97.7% at  $2 \cdot 10^6$  cycles are now nearly the same at sub-zero temperatures the difference to the tests at RT are still great. By looking at the knee point stress range  $S_k$  also a difference between the test results at sub-zero temperatures is observed. Moreover only very small changes in the slope and also in the band width of the scatter can be observed for sub-zero temperatures in comparison to the results with the method of linear regression. In comparison to that the slope at RT is less steep and the band width of the scatter smaller using the maximum likelihood method.

## 5 Further analyses of the test results

### 5.1 Fracture surface

As previous studies shows, the position of the crack initiation can have an influence on the fatigue strength of thermal cut edges. A distinction is made between cracks which appears at grooves in the thermal cut steel surface and cracks which appear at the corner of the cut edges and in case of post treated specimens at the chamfer. [10]

The crack growth can be traced by looking at the fracture surface. Thereby it is found that all fracture surfaces independent of the test temperature shows the same position for crack initiation. The crack initiation starts at the corner of the cut edges and initially continuous elastically until the specimen breaks. Figure 7 shows the fracture surface of specimens at test temperatures of  $-50^{\circ}\text{C}$  (a),  $-20^{\circ}\text{C}$  (b) and at RT (c).

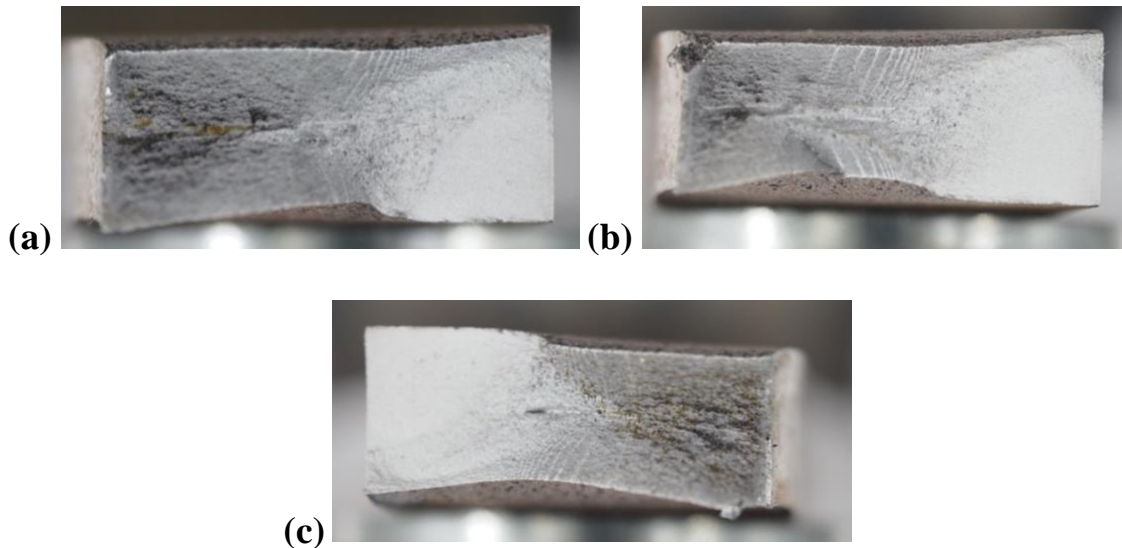


*Figure 7: Fracture surface of specimens tested at temperatures of  $-50^{\circ}\text{C}$  (a),  $-20^{\circ}\text{C}$  (b) and at RT (c).*

## 5.2 Crack position

Corners in the thermal cut steel surface can lead to local stress concentrations. As those stress concentrations can reduce the life time of a specimen significantly failure not only occur at half of the length of a specimen where the nominal stress is the highest [10]. Because of that the crack positions are measured and the nominal stress according to the local cross section is corrected. This procedure can lead to a sharp drop in the stress range when the crack location is relative far away from the middle. Because of this the statistical evaluation can become a problem in case single values deviate to much from the other. A outlier can occur if a specimen differs from the others. This can be a difference in shape but also changings in the test conditions. Such outliers lead to a very wide scatter band which represents the test results not correctly. To deal with such outliers a graphical analyses is used as there are no methods for a mathematical evaluation [3].

A outlier is found in the test results at  $-50^{\circ}\text{C}$ . In that case the crack originates 48 mm out of the middle of the specimen. Plotting the modified stress range of that test next to the S-N curve of the other 13 datapoints it becomes obvious that the value does not fit in the scatter band of the other values. This is shown in Figure 8. Thereby the statistical evaluation is conducted with the maximum likelihood method with optimization of the knee point. In case of the tests at  $-20^{\circ}\text{C}$  and RT such those outliers are not observed.

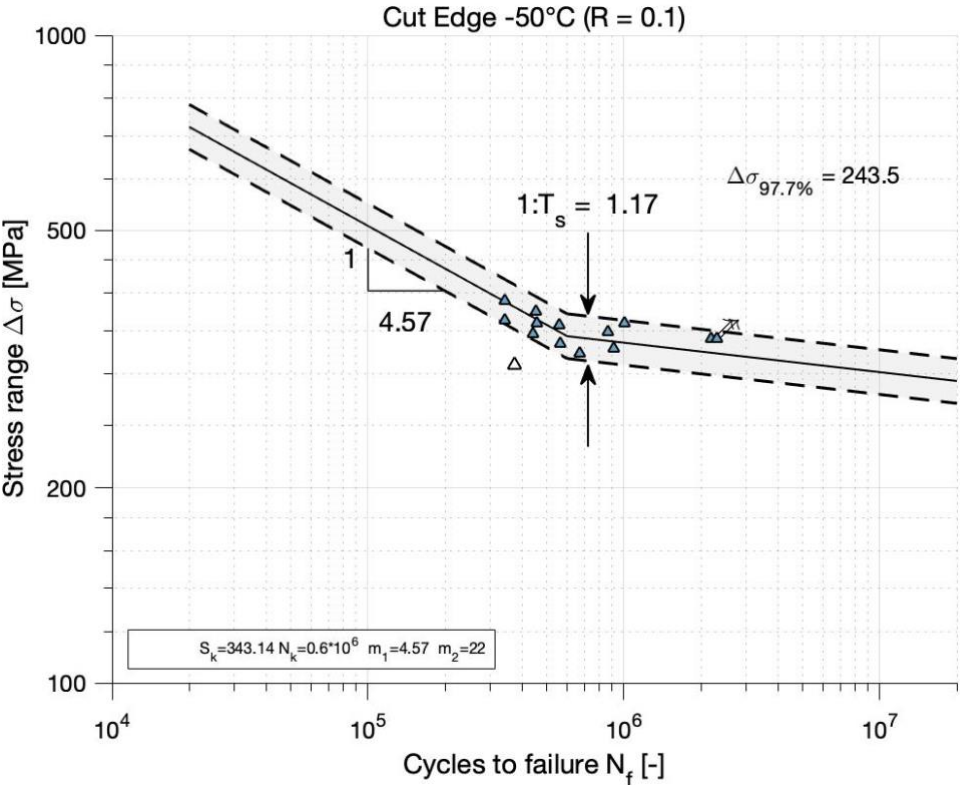


Figure 8: S-N curve for test results at  $-50^{\circ}\text{C}$  with modified stress ranges evaluated with the maximum likelihood method. The white triangle shows the outlier.

In all three of the modified S-N curves a decrease of the slope exponent is observed. Furthermore the knee point stress range for 50% survival probability is lower than in the evaluation with the original test data. But in total the difference of the fatigue strength between the sub-zero temperatures remain almost the same.

Next to the evaluation with the maximum likelihood method the linear regression is used here as well. Thereby it is observed that the slope differs even more to the results of the original test data. For example the slope of the results of the test series at  $-50^{\circ}\text{C}$  has decreased to  $m=3.84$  which is close to the recommended slopes in the guidelines of DNV ( $m=4$ ) [8]. All S-N curve parameters of all test series for both statistical methods are summarized in Table 2. The S-N curves with modified stress ranges for all test series can be find in the appendix.

Table 2: S-N curve parameter evaluated with linear regression and with maximum likelihood method for all test series

Statistical Method	Linear Regression			Maximum Likelihood Method					
	$m$	$1:T_s$	FAT [MPa]	$m_1$	$m_2$	$1:T_s$	$N_k$	$S_k$ [MPa]	FAT [MPa]
RT	3.75	1.5	189.1	5.21	22	1.31	$0.7 \cdot 10^6$	320.76	229.5
-20°C	5.65	1.1	252.9	6.05	22	1.1	$0.6 \cdot 10^6$	331.8	259.5
-50°C	6.82	1.17	277.3	5.3	22	1.12	$0.5 \cdot 10^6$	359.18	261.3
RT mod.	3.57	1.51	179.3	4.8	22	1.33	$0.7 \cdot 10^6$	310.11	216.5
-20°C mod.	5.12	1.12	237.9	5.26	22	1.13	$0.6 \cdot 10^6$	323.92	242.2
-50°C mod.	3.84	1.41	213.6	4.57	22	1.17	$0.6 \cdot 10^6$	343.14	243.5

### 5.3 Linear regression with constant slope

To get information about the fatigue performance of thermal cut edge steel at subzero temperatures the best fit S-N curves are evaluated using both described statistical methods. This procedure leads to different slopes for the different test series, which makes the comparison of values complicated because the difference of the test series depends on the cycles to failure. In order to nevertheless obtain information about the difference in the stress range, the linear regression is conducted with fixed slopes. For that the slopes are set to  $m=3$  like it is recommended by the IIW [1] and also  $m=4$  and  $m=3.5$  like it can find in the guidelines of DNV [8]. Then the FAT-class values of each test series is calculated with the fixed slopes. The results of the calculation and the corresponding FAT-class values from the guidelines for similar cases are shown in Table 3. [1, 8]

Table 3: FAT-class values for test series RT, -20°C and -50°C and for test series with modified stress range values with different fixed slopes and FAT-class values from guidelines [1, 8].

Test series	RT [MPa]	-20°C [MPa]	-50°C [MPa]	RT mod. [MPa]	-20°C mod. [MPa]	-50°C mod. [MPa]	Guideline (IIW case No. 122, DNV case B2 and C)
$m=3$	162	181.9	190.8	158.7	178.5	185.2	125 (IIW)
$m=3.5$	181	202.0	210.4	177.0	198.0	203.4	125 (DNV)
$m=4$	196.5	218.2	226.4	191.9	213.4	217.9	140 (DNV)

The increase in fatigue strength is represented by the increase in FAT-class values. In Figure 9 the percentage rise to the FAT-class value at RT for the different slopes are shown. Thereby

the increase is the greatest for a fixed slope of  $m=3$  and smallest for  $m=4$ . However for all used slopes a significant increase is observed.

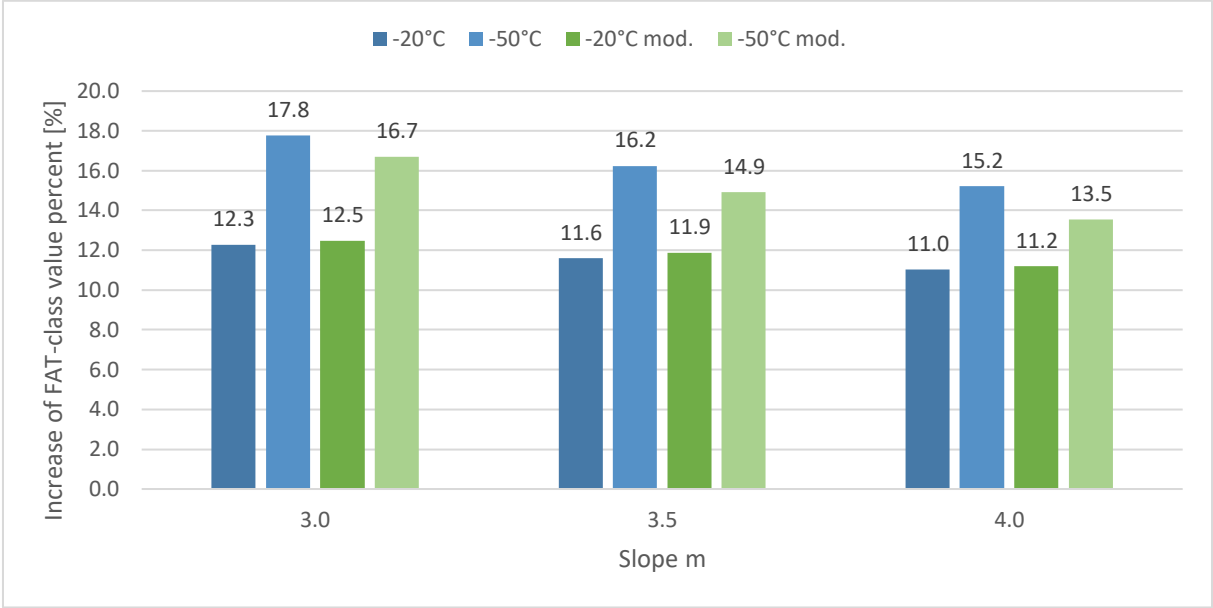


Figure 9: Increase of the FAT-class value in percent of original test series at sub-zero temperatures compared to RT and of modified test series compared to RT modified.

## 6 Discussion

Independent of the statistical method an increase in the fatigue strength of plasma cut specimens made of AH36 at subzero temperatures is observed. Despite this the results evaluated with the method of linear regression differs from them evaluated with the maximum likelihood method. Where the slope of the RT test series evaluated with the method of linear regression is much steeper as the slope of the test results of the sub-zero temperatures, the evaluation with the maximum likelihood method shows a less steep slope at RT which is closer to them of the tests at sub-zero temperatures. This is probably caused by the optimized knee point position and that the maximum likelihood method takes the runouts into account.

The difference in the statistical methods can also be observed by looking at the band width of the scatter. The tests at RT with the method of linear regression leads to a much wider scatter band as it is evaluated with the maximum likelihood method. This is also probably caused by the changed knee point position. In comparison to that the evaluation of the results of the sub-zero tests are not so much influenced by the type of statistical method. So the difference in the band width of the scatter is relatively small between both methods like it was also observed in case of the slope. However the maximum likelihood method seems to be better suited for the

comparison of the S-N curve parameters because no test series differs strongly from the others like it is in case of the RT test results with the method of linear regression.

The evaluation with the maximum likelihood method shows a difference in the fatigue strength of the three test temperatures at the knee point. But for the comparison of the fatigue strength the position of the knee point and the slopes of the curves has to be considered. This can be done by calculating the stress range of the  $-20^{\circ}\text{C}$  test series at the number of cycles where the  $-50^{\circ}\text{C}$  test series has its knee point. The stress range of the  $-50^{\circ}\text{C}$  test series at  $0.5 \cdot 10^6$  cycles to failure is then about 18 MPa greater than, the stress range of the  $-20^{\circ}\text{C}$  test series which is an increase of about 5%. Nearly the same difference in stress range can be observed at the knee points of the modified S-N curves between the tests at  $-20^{\circ}\text{C}$  and  $-50^{\circ}\text{C}$ . In that case the comparison of the knee point stress is easier as the optimized knee points are the same. But this kind of comparison is still full of uncertainties, as the difference in stress range between the test series depends on the cycles to failure. For example the FAT-class values of the test series  $-20^{\circ}\text{C}$  and  $-50^{\circ}\text{C}$  only differs about 2MPa. Because of that this way of comparison can only give information about the trend of the curves.

A better way to compare the stress ranges is to use fixed slopes for the evaluation with the method of linear regression. Through this the difference in fatigue strength can be evaluated at any position of the S-N curve. Using fixed slopes of  $m=3$ ,  $m=3.5$  and  $m=4$ , which are in the range of what the common guidelines like IIW or DNV recommend, an increase up to 17.8% for a fixed slope of  $m=3$  for the  $-50^{\circ}\text{C}$  test series without a stress range correction in comparison to the RT test series is observed. However, the slopes which are evaluated with the maximum likelihood method are less steep than  $m=3$ . Because of that a fixed slope of  $m=4$  seems to be better suited for this test series. In that case the increase from RT to  $-20^{\circ}\text{C}$  (11%) and to  $-50^{\circ}\text{C}$  (15.2%) is smaller but still significant. Considering the modified S-N curves where the stress range values are related to the cross section at the crack position the increase is for the tests at  $-50^{\circ}\text{C}$  smaller and for the  $-20^{\circ}\text{C}$  test series nearly the same than it is in the not modified data. In that case the comparison of the FAT-class values is especially well suited for the test series at RT and at  $-50^{\circ}\text{C}$  with fixed slopes of  $m=3.5$  and  $m=4$ , as the evaluated slopes with the method of linear regression are for both between this values. Then an increase from RT to  $-50^{\circ}\text{C}$  of about 13.5% for a slope of  $m=4$  and 14.9% for a slope of  $m=3.5$  is calculated.

The FAT-class values at RT, independent of the slope surpass the FAT-class values of the guidelines. As the test series of sub-zero temperatures shows an increase in fatigue strength this

underlines that the guidelines are very conservative especially for thermal cut edges at sub-zero temperatures.

From literature it is known that the fatigue of ferritic structural steel undergoes a ductile to brittle transition at the FTT which is related to a decrease in fatigue strength because the fatigue crack growth is accelerated. But the results of the fatigue tests shows that the fatigue strength of the tested thermal cut edges don't decrease up to the lowest test temperature of  $-50^{\circ}\text{C}$ . This is probably due to the fact that the transition takes place at lower temperatures than those tested in this thesis. A reference to that could be given by the fracture surfaces of the tested specimens, so it can be observed that all tested specimens failed in the same manner independent of the test temperature.

## 7 Conclusion

Thermal cut edge steel specimens of AH36 were tested at sub-zero temperatures and at room temperature. Then the best fit S-N curves were evaluated on one hand with the linear regression and on the other with the maximum likelihood method. Furthermore it was found that the cracks don't occur at the smallest cross section. Because of that the local nominal stresses at the actual crack position were calculated and the stress ranges corrected. With the modified data the statistical evaluation was repeated. For the comparison of the fatigue strength of the different test series and for the comparison with the guidelines the evaluation with the method of linear regression was also performed with fixed slopes for all test series, the modified and the not modified ones. The findings of this thesis are summarized in the following:

- Analysing the evaluated best-fit S-N curves, it is clear that the fatigue strength of the specimens which were tested at sub-zero temperatures, independent of the statistical method, increase in comparison to them, tested at room temperature.
- A fixed slope of  $m=4$  seems applicable for the evaluation with fixed slopes as the slopes which are found in the evaluation of the best fit S-N curves are close to that or a bit greater. The modification of the stress range leads to steeper S-N curves, which are even closer to a slope of  $m=4$ .
- Using fixed slopes makes the increase in fatigue strength even clearer. The highest increase in fatigue strength evaluated with a fixed slope of  $m=4$  is about 15.2% at a test temperature of  $-50^{\circ}\text{C}$  and in case of the modified data the increase is still about 13.5%.
- The comparison with the FAT-class values of the design curves of the common guidelines had shown that all test series surpass the FAT-class recommendations. This

shows that the design curves are very conservative for thermal cut edges especially at sub-zero temperatures.

- A difference in the crack location is not found. All cracks occur at the corner of the cut edges independent of the test temperature.
- It can be stated that untreated thermal cut steel edges of AH36 can be safely exposed to low temperatures down to  $-50^{\circ}\text{C}$ .

## References

- [1] Hobbacher A. Recommendations for fatigue design of welded joints and components, 2008; XIII-1823-07.
- [2] Braun M, Scheffer R, Fricke W, Ehlers S. Fatigue strength of fillet-welded joints at subzero temperatures. *Fatigue Fract Eng Mater Struct*. 2019;1-14.
- [3] Haibach E. Betriebsfestigkeit, Verfahren und Daten zur Bauteilberechnung. 2006. Springer-Verlag Berlin Heidelberg.
- [4] Merkblatt DVS 2403. Empfehlung für die Durchführung, Auswertung und Dokumentation von Schwingfestigkeitsversuchen an Schweißverbindungen metallischer Werkstoffe. Deutscher Verband für Schweißen und verwandte Verfahren. 2019.
- [5] Störzel K, Baumgartner J. Statistical evaluation of fatigue tests using maximum likelihood. Walter de Gruyter GmbH, Berlin/Boston. 2021.
- [6] Lipiäinen K, Ahola A, Skriko T, Björk T. Fatigue strength characterization of high and ultra-high-strength steel cut edges, *Engineering Structures* 228. 2021;111544.
- [7] Diekhoff P, Hensel J, Nitschke-Pagel T, Dilger K. Fatigue strength of thermal cut edges-influence of ISO 9013 quality groups. *Weld World* 63. 2019; 349–363.
- [8] DNVGL. Fatigue assessment of ship structures, 2015. DNVGL-CG-0129.
- [9] Schaumann P., Achmus M. Schlurmann T. et al. (2013). Report on Offshore Wind System Monitoring Practice and Normalisation Procedures, Marine Renewables Infrastructure Network.
- [10] von Bock und Polach F, Kahl A, Braun M, von Selle H, Ehlers S. (2019). Analysis of governing parameters on the fatigue life of thermal cut edges. *International Conference on Ships and Offshore Structures ICSOS*. 2019.
- [11] Braun M., Kahl A., Willems T., Seidel M., Fischer C., Ehlers S. (2021). Guidance for Material Selection on Static and Dynamic Mechanical Properties at Sub-Zero Temperatures, *Journal of Offshore Mechanics and Arctic Engineering*, Vol. 143 / 041704-13.

- [12] Von Bock und Polach F, Klein M, Kubiczek J, Kellner L, Braun M, Herrmring H. State of the art and knowledge gaps on modelling structures in cold regions. Proceeding of the ASME 2019 38<sup>th</sup> international conference on ocean, offshore and arctic engineering, 2019; Glasgow, Scotland, June 9-14.
- [13] Chatterjee A. (2018). Effect of Microstructure and Crystallographic Texture on Mechanical Properties of Modified 9Cr-1Mo Steel. Department of Metallurgical and Materials Engineering Indian Institute of Technology Kharagpur.
- [14] Walters C., Alvaro A., Johan M. (2016). The effect of low temperatures on the fatigue crack growth of S460 structural steel. International Journal of Fatigue 82 (2016) 110-118.
- [15] Braun M, Milaković A, Ehlers S, Kahl A, Willems T, Seidel M, Fischer C. Sub-zero temperatures fatigue strength of Butt-welded normal and high-strength steel joints for ships and offshore structures in arctic regions. Proceeding of the ASME 2020 39<sup>th</sup> International Conference on Ocean, Offshore and Arctic Engineering, 2020; Virtual, August 3-7.

# Appendix: Modified S-N curves

